

Determination of the saturated inductance of transformers by analytical formulae, comparison with an electromagnetic field calculation approach and validation by on-site tests.

Michel Rioual, *Senior Member, IEEE*, Yves Guillot, Cyrille Crépy

Abstract--This document describes the determination of the saturated inductance of a transformer, which is the slope of the saturation curve $\Phi(I)$ under highly saturated conditions.

This parameter, which has a strong impact on the overvoltages when energizing a transformer, has been determined from analytic formulae for a shell-type transformer.

Comparisons with the values derived from an electromagnetic 3D calculation and on-site tests are also given in this paper.

Index Terms--Energization, power transformers, inrush currents, saturated inductance, air-core inductance, core-type, shell-type.

I. NOMENCLATURE

L_{sat}	: saturated inductance of a transformer under highly saturated conditions	(H)
L_{aircore}	: air-core inductance of a transformer	(H)
L_{leakage}	: leakage inductance of a transformer winding	(H)
$\Phi(I)$: saturation curve of a transformer	(Wb)
N	: number of turns of a winding	(H)
Z_r	: reference impedance	(Ω)
S_r	: rated power	(VA)
U_r	: rated voltage	(V)
$L_{t,i}$: self-inductance of the turn i	(H)
$M_{t,ij}$: mutual inductance between the two turns i and j	(H)

For a shell-type transformer with pancake-type winding:

$M_{s,km}$: mutual inductance between the two sides k and m	(H)
$M_{s,km}(L,d)$: mutual inductance between the two equal sides k and m , which length is L and separated by the distance d	(H)
a	: width of a turn	(m)
b	: length of a turn	(m)
α, β	: dimensions of the section of a conductor	(m)
d_{ij}	: distance between the pancakes i and j	(m)
h_i	: radial thickness of the pancake i	(m)
t_i	: longitudinal thickness of the pancake i	(m)
N_i	: number of turns of the pancake i	

$C_{\phi/t}$: phase-to-ground capacitance of the overhead lines	(F)
Φ_n	: nominal flux in the transformer	(Wb)
Φ_{rA}	: residual flux in limb A	(Wb)
Φ_{rB}	: residual flux in limb B	(Wb)
Φ_{rC}	: residual flux in limb C	(Wb)
K_c	: coordination factor taking into account the accuracy of the calculation (e.g. discrete initial conditions) proposed in the IEC 71.1 standard.	
K_s	: aging factor associated to the insulation of the equipment, used in the IEC 71.1 standard.	
$L(\lambda)$: magnetization inductance including saturation	(H)
L_{I1}	: leakage inductance of the primary circuit	(H)
L_{I2}	: leakage inductance for the secondary circuit	(H)
L_{sat}	: last slope of the saturation flux-current curve	(H)
R_{Cu1}	: electric resistance of the primary circuit	(Ω)
R_{Cu2}	: electric resistance of the secondary circuit	(Ω)
R_{Fe}	: resistance describing the core losses	(\square)
S_N	: rated power of the target transformer	(MVA)
U_N	: nominal voltage of the EHV side of the target transformer	(kV)

II. INTRODUCTION

The energization of power transformers may create the saturation of the magnetic core and lead to high overvoltages and inrush currents. The magnitude of those stresses depends on the following different parameters:

- closing times of the circuit-breaker poles,
- residual fluxes in the core,
- transformer parameters as the winding connections, the hysteric curve of the magnetic core and the value of its air-core inductance.

This last parameter, which characterizes the slope of the saturation curve $\Phi(I)$ under highly saturated conditions, is deduced from the air-core inductance, as follows:

$$L_{\text{sat}} = L_{\text{aircore}} - L_{\text{leakage}} \quad (1)$$

Firstly, this paper describes the guiding principles of the analytical formulae giving the values of the air-core inductances, based on the determination of the sum of self and mutual inductances.

Secondly, analytical formulae have been determined for shell-type transformers with winding in pancakes.

M. Rioual is with EDF R&D, Clamart, 92140 France (e-mail: michel.rioual@edf.fr).

Y. Guillot is with EDF R&D, Clamart, 92140 France (e-mail: yves.guillot@edf.fr).

C. Crépy is with EDF R&D, Clamart, 92140 France.

Thirdly, the saturated inductance has been determined and applied to a 96 MVA transformer. The analytical approach has been compared:

- to the simulations made with a 3D electromagnetic field program;
- and to the value of the L_{sat} parameter determined by a comparison between on-site tests and EMTP simulations.

III. GENERAL PRINCIPLES OF THE ANALYTICAL CALCULATION OF THE AIR-CORE REACTANCE

The calculation of the air-core reactance of a transformer is mainly based on the calculation of sums of self and mutual inductances, derived from assumptions enabling those calculations.

From a theoretical point of view, it can be said that the self-inductance of a winding, constituted by two elements A and B in serie may be determined by making the addition of the self inductances of A and B, and also the double of the mutual inductance between A and B; extending those assumptions to a winding made of N turns, the air-core inductance may be derived as follows:

$$L_{aircore} = \sum_{i=1}^N L_{t,i} + \sum_{i=1}^N \sum_{\substack{j=1 \\ j \neq i}}^N M_{t,ij} \quad (2)$$

This is also described by the fig. 1 below:

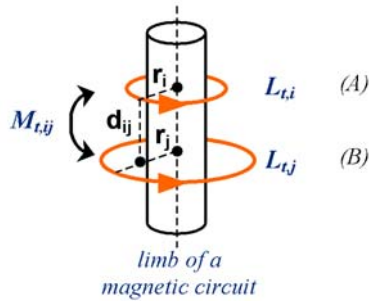


Fig. 1. Interaction between the two turns i and j , for a core-type transformer.

The exact theoretical calculation of the mutual between two circular turns has been described by Maxwell [1], [2], and is based on elliptical integrals derived from the Neumann's formula. Those approaches are at the origin of those generally used by manufacturers for the calculation of air-core inductances.

IV. DETERMINATION OF THE AIR-CORE REACTANCE FROM ANALYTICAL FORMULAE FOR A SHELL-TYPE TRANSFORMER

A. Description of the approach

The shell-type technology makes the calculation of air-core inductance from analytical formulae more complex, because of the rectangular form of the turns, as described on fig. 2 below.

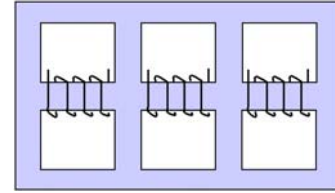


Fig. 2. Magnetic circuit for a shell-type transformer.

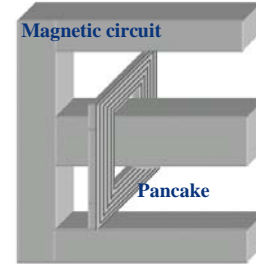


Fig. 3. 3D-view of a shell-type transformer with windings in pancakes.

The proposed analytical approach consists in subdivising the HV winding in well chosen parts so that self and mutual inductances could be calculated with accurate formulae:

- The self-inductances of one pancake is obtained by calculating, for each turn, the self-inductance and the mutual inductances with the other turns, and then by summing all those values. The mutual inductance between two turns is calculated from the sum of the different sides of both rectangles.
- The mutual inductance between two pancakes is obtained by summing all the mutuels corresponding to each couple of turns from two different pancakes.
- The global self-induction is the sum of selfs and mutuels of every couple of pancakes.

The insulation and the rounded edges of the pancakes are not taken into account in this approach.

The self-inductance $L_{t,i}$ of a single turn i is given by the following formula [3]:

$$L_{t,i} = 10^{-9} \cdot 4 \cdot \left((a+b) \cdot \log \left(2 \frac{a \cdot b}{\alpha + \beta} \right) - a \cdot \log(a+d) - b \cdot \log(b+d) - \frac{a+b}{2} + 2d + 0.447(\alpha + \beta) \right) \quad (3)$$

with $d = \sqrt{a^2 + b^2}$.

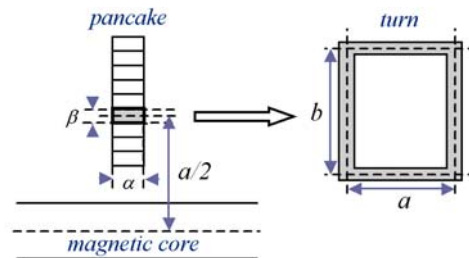


Fig. 4. Geometrical dimensions of a turn.

The mutual inductance between two orthogonal sides is equal to zero. The mutual inductance $M_{s,nq}$ between two parallel sides separated by a distance d (see parameters on fig. 5) is deduced from mutual inductances, noted

$M_{s,n'q}(L,d)$, between two parallel equal sides of appropriate length L and separated by the distance d [3].

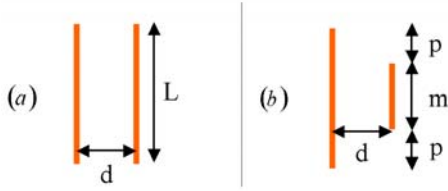


Fig. 5. Parameters of the mutual inductance in the following cases: two parallel equal sides (a), two parallel unequal sides (b).

The mutual inductance between two parallel equal sides (case (a) in the fig. 5) n and q of length L is given by the following formula:

$$M_{s,nq}(L,d) = 10^{-9} \cdot 2L \cdot \left(\ln \left(\frac{L}{d} + \sqrt{1 + \frac{L^2}{d^2}} \right) - \sqrt{1 + \frac{d^2}{L^2}} + \frac{d}{L} \right) \quad (4)$$

The mutual inductance between two parallel unequal sides (case (b) in the fig. 5) n and q can be deduced from the previous formula as follows:

$$M_{s,nq} = M_{s,n'q}(m+p,d) - M_{s,n'q'}(p,d) \quad (5)$$

Considering geometrical symmetries, the mutual inductance between two turns can be calculated from the mutual inductances between the parallel sides of the two rectangles [3], as follows:

$$M_{t,km} = 2(M_{s,15} - M_{s,17} + M_{s,26} - M_{s,28}) \quad (6)$$

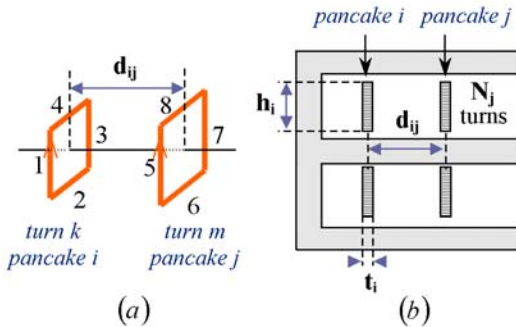


Fig. 6. Parameters of inductive coupling between: two turns (a), two pancakes (b).

B. Application to a 96 MVA auxiliary transformer

This analytical approach has been applied to a 96 MVA auxiliary transformer of a 1300 MW thermal power plant. It consists of a 400 kV/6.8 kV shell-type transformer, with pancakes type windings, made of 960 turns for the HV one.

The calculation has led to a value of 0.22 p.u. for the air-core inductance, this value being 17% under the value of 0.26 p.u. given by the manufacturer (see Table 1) with an accuracy of 20%.

A comparison with an electromagnetic 3D software is given in chapter 4.

TABLE I

COMPARISON BETWEEN THE ANALYTICAL APPROACH DEVELOPED AND THE VALUE GIVEN BY THE MANUFACTURER, FOR THE 96 MVA TRANSFORMER.

Analytical approach for shell-type transformers	Manufacturer value
$L_{\text{aircore}} = 1.157 \text{ H}$ (0.22 p.u.)	$L_{\text{aircore}} = 1.4 \text{ H}$ (0.26 p.u.)

The mutual inductances between pancakes represent around 85% of the global air-core inductance.

V. COMPARISON BETWEEN THE ANALYTICAL APPROACH AND AN ELECTROMAGNETIC 3D CALCULATION (SINGLE-PHASE AND THREE-PHASE SIMULATIONS)

A. Description of the 3D approach

The results of the analytical approach have been compared to the simulations performed with the electromagnetic 3D software “FLUX3D”. It enables, in particular, the calculation of the 3D magnetic field developed in the transformer and requires a 3D geometrical meshed model of the transformer (see Fig. 7).

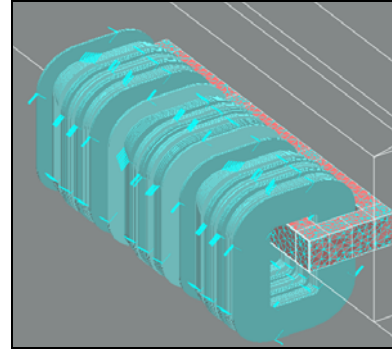


Fig. 7. Model of a shell-type transformer in FLUX3D.

The FLUX3D approach has been applied to the shell-type transformer previously mentioned. The relative permeability μ_r is set to 1 in order to meet very high saturation requirements faced during the energization. The simulations were performed in steady state conditions, first in a single-phase mode, secondly in a three-phase mode, in order to evaluate the mutual inductances between phases. The transformers were supposed to be no-loaded, which is the case during their energization.

Considering the results given by FLUX3D, the air-core inductance can be determined from three equivalent ways: the calculation of the energy, the determination of the impedance or the calculation of the magnetic fluxes.

B. Case of a single-phase simulation

The FLUX3D single-phase approach was applied to the determination of the air-core reactance for the shell-type 96 MVA transformer. Its high voltage and middle voltage windings are connected in serie.

The three-phase coupling is a wye one for MV-HV windings, a delta connection for the LV winding.

In the simulation, a single MV-HV phase was energized, no matter which phase it was because of the symmetry, and other windings were all left open.

From the results given by FLUX3D, the three methods (either energy, impedance, or flux) give 1.21 H as value of the air-core inductance for the 96 MVA transformer.

C. Influence of the mutual inductances: results of three-phase simulations for two technologies

As the energization of a transformer is a three-phase operation, the inductive coupling between phases slightly modifies the slope of the saturation curve $\Phi(I)$, compared to the single-phase case. The coupling phenomena can be represented by mutual inductances between phases.

To take into account the mutual-induction between phases and to estimate its influence on $L_{aircores}$, three-phase simulations have been performed on the shell-type 96 MVA transformer, in steady state conditions, with no-load conditions at the secondary side and in the following conditions:

- three-phase power conditions,
- presence of the low voltage required, as its delta coupling enables induced currents.

The air-core inductance for the middle phase is the highest one, due to the geometrical proximity with both windings of phases 1 and 3, which leads to higher mutual induction coefficients.

In the case of the shell-type 96 MVA transformer, the FLUX3D approach has led to a value of 1.219 H (0.23 p.u.) for phase 1.

This value is 5% higher than the value of 1.157 H (0.22 p.u.) calculated by the analytical approach for shell-type transformers presented in chapter 3. The value provided by the manufacturer is equal to 0.26 p.u.

It must be noticed that the determination of the air-core reactance by the FLUX3D approach requires several hours for the modeling of the transformer and simulations to be performed. For the analytical approaches developed, the calculation time essentially depends on the number of turns and the technology.

It remains less than 5 mn for a 960 turns (per HV phase) pancake-type winding of a shell-type transformer, with a ~2 GHz processor.

VI. VALIDATION BY COMPARISON WITH ON-SITE TESTS

A. Description of the network and modelling of the equipment.

The 96 MVA transformer energization has been studied in real conditions, matching the process used for the re-energization of thermal plants in some cases after a blackout.

The complete network has been modelled, with the 96 MVA transformer, energized from a 900 MW thermal plant through a long line of 133.6 km. This network is shown in figure 8, the circuit-breaker from which the transformer is energized is located in the substation of the thermal plant, 1 km from the transformer:

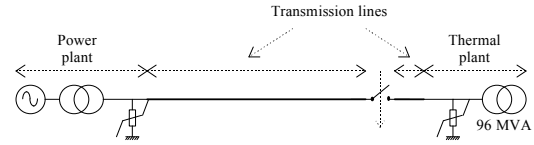


Fig. 8. Description of the 400 kV network.

The power plant includes a 1120 MVA generator followed by a 1080 MVA step-up power transformer.

The network equipments have been represented under the phenomena being involved, as follows:

- the 900MW generator is represented by an sinusoidal voltage source behind its subtransient reactance X''_d impedance and the damping derived from the time constant T''_d , those parameters being given by the manufacturer.
- the 1080 MVA shell-type step-up transformer is modeled by a three single-phase transformers where the leakage reactances, the copper and core losses and the saturation are taken into account. The coupling is represented $Y_{nd_{1,1}}$ with its grounding reactance of 25 Ω and its surge arrester. The resistance values are increased in order to take into account the eddy currents and skin effects.

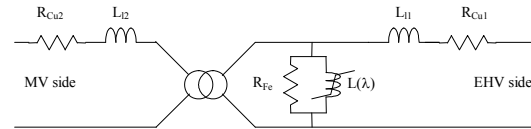


Fig. 9. Description of the transformer diagram (one phase).

- the zinc oxide surge arresters, having a rated voltage of 360 kV are represented by their non-linear resistance [9].
- the overhead lines are described by PI cells, the R, L, C parameters being derived from the electrical and geometrical parameters given by the Transportation Division using an auxiliary routine of the EMTP program. The number of PI cells has been chosen to 10 in order to represent correctly its exact impedance under the fifth harmonic which is the resonance frequency of this network (see figure 9),
- the corona effect affecting the overhead lines is also represented, by non-linear resistances inserted along the PI cells [5]. Their parameters describing the losses are derived from the ratio between the electrical field generated by the wires over the Peek's critical field.
- the target 96 MVA transformer with its triangle coupling at the secondary side is modeled like the previous one [4] except that the hysteretic curve is completely represented. The saturation is built from the voltage-current curve [6] given by the manufacturer. The parameter L_{sat} , describing the slope of this curve under extreme saturated conditions, is fixed at 0.16 p.u.⁽¹⁾, equal to 0.89 H, in order to be conservative. The manufacturer has proposed 0.20 pu with an accuracy of 20 %, taking into account that the value is not well defined, the transformer being only tested under low saturation conditions.

Note ⁽¹⁾: The L_{sat} in p.u. is derived from the one in Henry by the following expression:

$$L_{sat}(p.u.) = L_{sat}(H) \frac{S_r \omega}{U_r^2} \quad (7)$$

From the real on site tests performed, it has been possible to determine a resonant frequency of 240 Hz of the upstream network [10]. A frequency scan performed with this EMTP program has then been performed on the entire network, as shown below, figure 10 describing the direct impedance, a three-phase current source replacing the saturation part of the target transformer in order to get the equivalent impedance of the network :

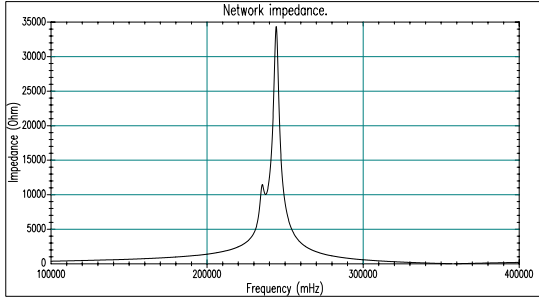


Fig. 10. Direct impedance versus frequency of the 400 kV network.

It shows a resonance close to the fifth harmonic (244 Hz), the zero impedance being characterized by a frequency of 491 Hz.

B. Description of the 96 MVA transformer energization and determination of the L_{sat} parameter by comparison between on-site tests and simulations with the EMTP program

B.1 On-site tests

On site tests have been performed by the Technical Transportation Division of EDF, his 96 MVA transformer has been energized [11] from the power plant.

An acquisition system has been installed in the substation and especially on the circuit breaker. Phase-to-ground voltages and inrush currents have been measured from the on site dividers (voltage and current transformers) located in the substation. The outputs of the dividers are connected to the central acquisition system. All electrical values have been digitized at the sampling rate of 400 Hz and processed in order to be used with a software (Matlab).

B.2 Determination of the initial conditions associated to the on-site tests

They are determined as follows :

- the closing instants of the breaker are obtained from the measurements performed on the inrush currents. For each phase, the closing instant is located when the current of the same pole becomes non negative. In the case of those on-site tests, they are 2, 7 and 7 ms for phase A, B and C respectively. The 0 ms is defined when there is a zero-crossing of the positive wavefront of the phase A-to-ground voltage, introducing a same reference for the measurements and the simulations.
- the residual fluxes are derived from the integration of the phase-to-ground voltages of the transformer (secondary side at 6,8 kV) after the opening of the circuit breaker. In the case of this test, the measured residual fluxes are 0, -75 and 75 Wb in the limbs of phases A, B and C

respectively. That represents about 7 % of the nominal flux of this transformer.

The purpose of the following part is to assess the network parameters X_d'' , $C_{\square/t}$ and the L_{sat} slope of the saturation curve of the target transformer within their accuracy boundaries and, then, compare the results between the on-site measurements and the simulations.

B.3 Determination of the resonant frequency of the network

The resonance frequency of the network has been performed by the mean of a Fourier analysis triggered immediately after the energization and made on the measured phase-to-ground voltages.

A frequency scan of the network with its standard parameters determines the resonance frequency of the phases A, B and C at 244.1 Hz, 235.8 Hz and 238.6 Hz respectively, implying an average resonance frequency of 239.5 Hz.

The resonance frequency of the simulated network shows that the discrepancy is 7.5 Hz compared to the measured frequency. Since these parameters X_d'' and $C_{\square/t}$ are known within an accuracy of 15 % and 5 % respectively, the resonance frequency of the simulated network may reach the measured one when increasing X_d'' and $C_{\square/t}$ by 11 % and 5 %. In that case, these frequencies decrease to 235.2 Hz, 226.5 Hz and 229.2 Hz respectively.

The average value is therefore 230.3 Hz which is inside the accuracy range of the measured frequency with these determined parameters.

B.4 Determination of the slope L_{sat} of the saturation curve $\square(I)$ for the target transformer

During the first times (periods of 50 Hz) immediately after the closing of the breaker, the inrush currents mainly depend on the saturation curve of the target transformer [7] [8] and especially on the L_{sat} slope of this curve.

With a L_{sat} equal to 0.16 p.u. (conservative side), the maximum amplitude is reached for the pole A which implies a maximum deviation of 21.5 %, the simulations computing 333 A instead of 274 A measured.

If this last value is set to 0.21 p.u. which is in the accuracy boundaries (0.20 pu \pm 20 %) given by the manufacturer, the deviations reach their minimum values, as shown in table 2 below:

TABLE II
COMPARISON OF THE MAXIMUM AMPLITUDES OF THE INRUSH CURRENTS BETWEEN SIMULATIONS AND MEASUREMENTS FOR L_{SAT} EQUAL TO 0.21 PU.

	Phase A	Phase B	Phase C
Measured	274 A	161 A	342 A
Simulated	280 A	139 A	327 A
Deviation	2.2 %	13.7 %	4.4 %

The maximal amplitude of the inrush currents are 274 A, 161 A, 342 A for phases A, B and C respectively, as shown in figure 11 for phase B.

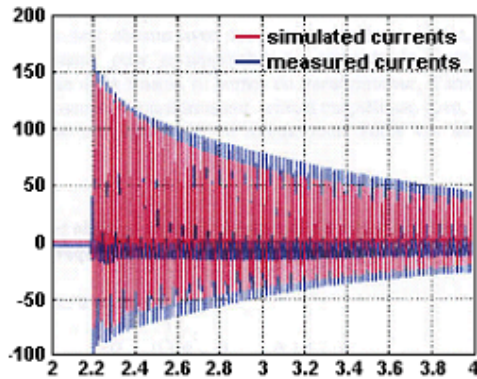


Fig. 11. Comparison between simulated and measured currents for phase B.

This value of 0.21 p.u. for the air-core inductance is very close to the one previously determined by the analytical approach gives 0.19 p.u. for the L_{sat} parameter, and leads to a good agreement between the simulated and measured currents (see fig. 11).

VII. DISCUSSION

The air-core inductance is not, in most cases, a key parameter for manufacturers, which are more focused on short-circuit issues from the specifications required by utilities. They often provide a value for the air-core reactance, generally calculated by approximate formulae using a global geometry of the transformer (envelope of the winding), with a 10 to 20% accuracy.

For utilities, the L_{sat} value is highly critical for certain studies, because a 10% surestimation of the L_{sat} can lead to underestimate stresses during the transformer energization by a factor of 30%. The analytical approaches developed in this paper enable an improvement of the L_{sat} values, with a better accuracy than those given by more simple approaches.

VIII. CONCLUSION

This document describes the determination of the saturated inductance of a shell-type transformer, in order to improve the value given by the manufacturer.

This parameter, which has a strong impact on the overvoltages when energizing a transformer, has been determined from analytic formulae for shell-type transformers.

A comparison with the values derived from an electromagnetic 3D calculation is also given in this paper. Applied to a shell-type 96 MVA transformer, both approaches have shown a good agreement. A simulation in EMTP with the value of L_{sat} analytically calculated has shown a good agreement between the simulated and measured currents.

IX. REFERENCES

- [1] J. C. Maxwell "Treatise on Electricity and Magnetism", Editions Jacques Gabay, 1887, Paris.
- [2] E. B. Rosa, F. W. Grover, "Formulations and tables for the calculation of mutual and self-induction [Revised]", Washington Government Printing Office, 1911, from Bulletin of the Bureau of Standards Vol. 8 N°1.
- [3] F. W. Grover, "Inductance Calculations: Working Formulas and Tables", 1946 & 1973, Dover Phoenix Edition, 2004.
- [4] A. Narang, R.H. Brierley, "Topology based magnetic model for steady-state and transient studies for three-phase core type

- transformer", IEEE Transactions on Power Systems, Vol. 9, No. 3, August 1994.
- [5] G. Sybille, M.M. Gavrilovic, J. Bélanger, "Transformer saturation effects on EHV system overvoltages", IEEE Transactions on Power Apparatus and Systems, Vol. PAS-104, No. 3, March 1985.
- [6] W.L.A. Neves, H.W. Dommel, "Saturation curves of delta-connected transformers from measurements", IEEE, No. 94 SM 459-8 PWRD, July 1994.
- [7] J.H.B. Deane, "Modeling the dynamics of the nonlinear inductor circuits", IEEE Transactions on Magnetics, Vol. 30, No. 5, September 1994.
- [8] C. Kieny, K. Ben Driss, B. Lorcet, "Application of a disturbance method to the continuation of sub-harmonic and harmonic regimes in parallel ferroresonant circuits", Collection de notes internes de la Direction des Etudes et Recherches, No. 94NR00033, 1994.
- [9] N. Nenemenlis, M. Ené, J. Bélanger, G. Sybille, L. Snider, "Stresses in metal-oxide surge-arresters due to temporary harmonic overvoltages", Electra, No. 130.
- [10] GT 33.10/WG 33.10, "Temporary overvoltages withstand characteristics of extra high voltage equipment", Electra, No. 179, August 1998.
- [11] M. Rioual, C. Sicre, "Energization of a no-load transformer for power restoration purposes: Modelling and validation by on site tests." *IEEE Volume 3, 2000, Jan. 23-27, Page(s):2239-2244*.

X. BIOGRAPHIES

Michel Rioual was born in Toulon (France) on May 25th, 1959. He received the Engineering Diploma of the "Ecole Supérieure d'Electricité" (Gif sur Yvette, France) in 1983. He joined the EDF company (R&D Division) in 1984, working on electromagnetic transients in networks until 1991. In 1992, he joined the Wound Equipment Group as Project Manager on rotating machines. In 1997, he joined the Transformer Group, as Project Manager on the transformers for nuclear plants. He is a Senior of IEEE, belongs to CIGRE and to the SEE (Society of Electrical and Electronics Engineers in France).

Yves Guillot was born in Paris, France, on April 1st, 1967. He received his Electrical Engineering diploma of the "Ecole Supérieure d'Electricité" (Supélec) in 1990. Then he joined the research center of EDF as a research engineer mainly involved in modeling power transformers : high frequency modeling, diagnosis methods and electromagnetic field calculation.

Cyrille Crépy was born in Paris on June 30th, 1986. He received the Engineering Diploma of the "Ecole Supérieure d'Electricité" (Gif sur Yvette, France) in 2008. He gathered his first work experience during internships at the nuclear power plant of St-Laurent-des-Eaux, and MBDA. He completed his studies by a 6 months internship at EDF R&D where he worked on stresses during transformers energization.